Hindawi
Advances in Materials Science and Engineering
Volume 2021, Article ID 5541587, 14 pages
https://doi.org/10.1155/2021/5541587

Research Article

Influence of Cross-Sectional Shape on the Mechanical Properties of Concrete Canvas and CFRP-Reinforced Columns

Jiangang Niu,[1] **Wenming Xu**,[1] **Jingjun Li**,[1] **and Jian Liang**[2]

[1]*Department of Civil Engineering, Inner Mongolia University of Science and Technology, Baotou 014000, China*
[2]*Department of Civil Engineering, Guangxi University, Nanning 530000, China*

Correspondence should be addressed to Wenming Xu; 2018022102@stu.imust.edu.cn

Received 2 February 2021; Revised 11 April 2021; Accepted 26 April 2021; Published 12 May 2021

Academic Editor: Ivan Giorgio

Fiber-reinforced polymer (FRP) wrapping has become an attractive strengthening technique for concrete columns. However, the ingress of corrosion into the concrete through the gap of CFRP fiber greatly reduces the durability of concrete and the bearing capacity of specimens. Concrete canvas, a kind of corrosion-resistant and refractory material, is a promising method to enhance durability and carrying capacity. In this study, the concrete canvas (CC) and carbon fiber-reinforced polymer (CFRP) were used to jointly reinforce columns with square cross section, octagonal cross section, circular cross section, and elliptical cross section. The influence of section shape on the strengthening effect of the axial compression column was investigated by the axial compression test. The results showed that the section shape had a significant influence on the reinforcement effect of the axial compression column. The carrying load capacity and ductility coefficient of different columns follow this order: square column < oval-shaped columns < octagonal columns < circle columns. The increased amplitude of bearing capacity for the different columns with the increase of CC layers follows this order: square columns < oval-shaped columns < circle column < octagonal columns. Compared with the unconstraint columns, the bearing capacity of adopting two-layer CC columns increased by 129%, 155%, 150%, and 139% for the square, octagonal, circular, and elliptical columns, respectively. The octagonal column has the largest increase range. Compared with the unconstraint columns, the bearing capacity of adopting two-layer CC columns increased by 348%, 318%, 310%, and 296% for the square, octagonal, elliptical, and circular columns, respectively. The square column has the largest increase range. The stress concentration phenomenon of all section shapes was weakened after the CC was used. The application of the CC on CFRP-reinforced columns improves column ductility significantly, with some degree of increase in bearing capacity.

1. Introduction

More recently, CFRP has been used frequently in the reinforcement of various components, mainly because they have better mechanical properties and corrosion resistance than traditional building materials [1–8]. However, adverse conditions (e.g., sulfate, chloride, temperature, humidity, or acidic environments) are capable of undermining the integral property of CFRP-enhanced concrete structure, as well as noticeably impacting the FRP-to-concrete bonded interface's behavior and failing mechanisms [9]. Besides, the corrosive substances can erode into the interior of the column through the gap in harsh environments because the CFRP sheet is made up of crisscrossed fibers [10]. Moreover, degradation of the column wrapped with CFRP mechanical characteristics is likely to appear for being exposed to a harsh environment. Soudki [11] demonstrated that CFRP can be wrapped to reduce the corrosion degree of the member and improve its durability, but there are different degrees of damage through electrochemical corrosion of CFRP-reinforced concrete members. Kim and Ji [12] showed that CFRP entanglements disrupted the penetration of acids into the core concrete and impeded chemical reactions based on concrete-acid reactions. However, the CFRP wrapping becomes less effective as the acid exposure period is extended, and the compressive strength and ultimate axial strain of the restraint column are significantly reduced. Although there have been some studies on the influence of severe

environmental conditions on CFRP-reinforced concrete structures in recent years [13–15], the research has been rare on the way to resist corrosive substances with new material. Concrete canvas refers to the most hopeful product of engineering utilization of 3D spacer fabric reinforced cementations composites [16, 17]. Concrete canvas [18–20] has extensive application in ditch lining and slope protection projects due to its high impermeability, durability, environmental benefits, fire resistance, and chemical corrosive resistance. At present, most scholars focus on the research of concrete canvas itself. Zhang [21] researched the enhancement of CC panels' tensile and flexural strengths by outer reinforcement using a fiber-reinforced polymer (FRP) sheet. As revealed from the mentioned outcomes, the mechanical characteristic of FRP-reinforced CC is noticeably enhanced. Nevertheless, there are few pieces of research studies that focused on the reinforced members with CC.

Studies on CFRP confined columns' characteristics primarily discussed circular columns, whereas rare studies focused on octagonal, square, and elliptical columns [22, 23]. The partial reason for such result is that CFRP-reinforced octagonal, square, and elliptical sections have no uniform confinement with not evenly distributing compressive pressure [24, 25]. Nevertheless, rectangular columns have a wide range of applications in building structure construction. Moreover, octagonal and elliptical shapes are constructed due to various needs, such as beautiful appearance, reasonable layout, and performance requirements [26, 27]. Accordingly, for preserving the integral property of infrastructures, their strength and rehabilitation should be highlighted [28, 29]. Besides, a large number of scholars have carried out extensive research on the influence of column section shape change on the reinforcement effect [23–28]. Yan [30] has demonstrated that the elliptical shape and the circular shape cross section can better exert the tensile strength of the fiber material by the axial compression test of the rectangular section, the rectangular chamfered section, the rectangular modified ellipse section, and the circular section column. Wang [31] showed that the angular radius rate is proportional to the rise of the strength of the limited concrete by testing the CFRP-wrapped concrete short column with different corner radii. Al-Salloum [32] has demonstrated that the process to smooth square cross-sectional edges is critical to delaying FRP composite's rupture at the mentioned edges through the axial compression test of the 20 specimens that varied from square to circular. Farghal [33] delved into the section length-to-width ratio's impact on the structural ductility and strength of the constrained column. As revealed by the outcome, the aspect rate noticeably impacts the strength increase, whereas it slightly impacts the ductility. Jameel [34] found that the cyclization technology reduced the stress concentration at the corner and improved the ultimate ductility and bearing capacity by circularizing the hollow column and the solid column. According to the above studies, the cross-sectional shape of the column has a close association with the bearing capacity and ductility of the CFRP-reinforced column.

Based on the above analysis, this study provides new reinforcement insights (CC and CFRP joint reinforcement) to improve the mechanical properties and durability of reinforced columns. The study in this article comprehensively investigates the improvement of the mechanical behavior of CC and CFRP reinforcement for different cross-sectional shapes. It can provide a basis for the application of this reinforcement technology in practical engineering.

2. Experimental Procedure

2.1. Specimen Design. For the investigation of the influence exerted by variation cross-sectional shape on columns reinforced by CC and CFRP, forty-four test columns with the same cross area were developed. Table 1 gives the experiment-based matrix. We used 3 variables, including four cross-sectional shapes (circle, square, octagon, and ellipse), two kinds of reinforced method (CFRP, CC and CFRP), and two CC layers (1-layer, 2-layer). All specimens had a height of 450 mm. Each specimen has three nominally identical samples. Without special description, all the results are the best values of the three sets of nominal samples. Figure 1 presents the schematic of the reinforced column dimensions. To facilitate analysis, the test pieces are divided into three series. Among the three series, series I were reinforced by CFRP and series II were reinforced by CC and CFRP.

2.2. Fabrication of Specimens. Before jacketing, the specimens' surface underwent a light sanding process for the removal of surface pollutants, water cleaning process, and drying process. Subsequently, the 2-part epoxy impregnation resin underwent thorough mixing following the producer's rules. For columns only reinforced by CFRP, we employed a thin resin layer on the sample's surface firstly; next, the CFRP laminate received careful wrapping process over the sample with the fibers following the hoop orientation for forming 1 or 2 CFRP layers. No void existed between the CFRP and the concrete surface, which was ensured. When the wrapping process was achieved, the gap between the top/bottom of the concrete specimen and the FRP was downregulated to nearly 10 mm. For ensuring the FRP jacket's overall tensile strength, a 100 mm long overlapping zone between the starting part and the achieving part of the respective sheet was enabled. For columns reinforced by CC and CFRP, we added anhydrite and CSA to a mixer and blended them for 10 min at 94 r/min firstly. Subsequently, the powder mixture was progressively arranged and underwent vibration in the mold with 3D spacer fabric till the 3D spacer fabric reached complete impregnation by powder. Next, a membrane is covered with the CC surface to avoid the cement powder falling out during the wrapping process. The CC is slowly wrapped on the column and fixed with nylon tape, and then, water is sprayed while uncovering the membrane. The water quantity is calculated by the amount of cement to ensure the complete hydration of cement. The second layer of CC is wrapped in the same way as the first layer of CC after the first layer of CC is hardened. Finally, we employed CFRP laminates to the sample's surface, and the jacketing procedure is the same with columns only reinforced by

Table 1: Experimental matrix of specimen parameters.

Series	Specimen	Cross-sectional shape	Height (mm)	CC layers	CFRP layers	CC thickness (mm)
/	S-0-0-1 S-0-0-2	Square	450	0	0	0
	O-0-0-1 O-0-0-2	Octagon	450	0	0	0
	C-0-0-1 C-0-0-2	Circle	450	0	0	0
	E-0-0-1 E-0-0-2	Ellipse	450	0	0	0
I	[a]S-0-1-1 S-0-1-2 S-0-1-3	Square	450	0	1	0
	O-0-1-1 O-0-1-2 O-0-1-3	Octagon	450	0	1	0
	C-0-1-1 C-0-1-2 C-0-1-3	Circle	450	0	1	0
	E-0-1-1 E-0-1-2 E-0-1-3	Ellipse	450	0	1	0
II	S-1-1-1 S-1-1-2 S-1-1-3	Square	450	1	1	20
	O-1-1-1 O-1-1-2 O-1-1-3	Octagon	450	1	1	20
	C-1-1-1 C-1-1-2 C-1-1-3	Circle	450	1	1	20
	E-1-1-1 E-1-1-2 E-1-1-3	Ellipse	450	1	1	20
III	S-2-1-1 S-2-1-2 S-2-1-3	Square	450	2	1	40
	O-2-1-1 O-2-1-2 O-2-1-3	Octagon	450	2	1	40
	C-2-1-1[b] C-2-1-2 C-2-1-3	Circle	450	2	1	40
	E-2-1-1 E-2-1-2 E-2-1-3	Ellipse	450	2	1	40

Notes:[a]1. "S" represents the square section shape concrete. "O" represents the octagon section shape concrete. "C" represents the circle section shape concrete. "E" represents the ellipse section shape concrete.[b]2. Taking "C-2-1-1" as an example, the letter "C" denotes the circle section shape concrete. the number "2" is the layer of CC, the number "1" is the layer of CFRP, and the last number "1" represents the nominal same sample.

CFRP. Figure 2 shows the columns after coating with CFRP or CFRP and CC.

We kept samples at ambient temperature for no less than 7 days before testing for ensuring sufficient curing time of the epoxy. Before the samples were loaded to the test machines, the ends of the jacket underwent the grinding process smoothly for the removal of any uneven edge.

2.3. Material Properties. Table 2 lists the quantities of ingredients in the concrete mix. The FRP tensile test is tested following what is specified by the ASTM D3039 standard [35]. The carbon fiber reinforcement polymer (CFRP) employed in the present article for strengthening the concrete specimens displayed a tensile strength of 3547 MPa and a modulus of elasticity of 2.33×105 MPa. The thickness per layer reached 0.167 mm. Table 3 presents the mechanical properties of CFRP. A two-part epoxy impregnation resin acted as the adhesive. Table 4 presents typical mechanical characteristics of epoxy resin. The CC strength is tested following what is specified by the JCJ/T 70–2009 [36] standard. Considering the limitation of CC thickness, the CC is cut into 20 mm × 20 mm × 20 mm cubes for the test. Table 5 presents the mechanical properties of CC. The

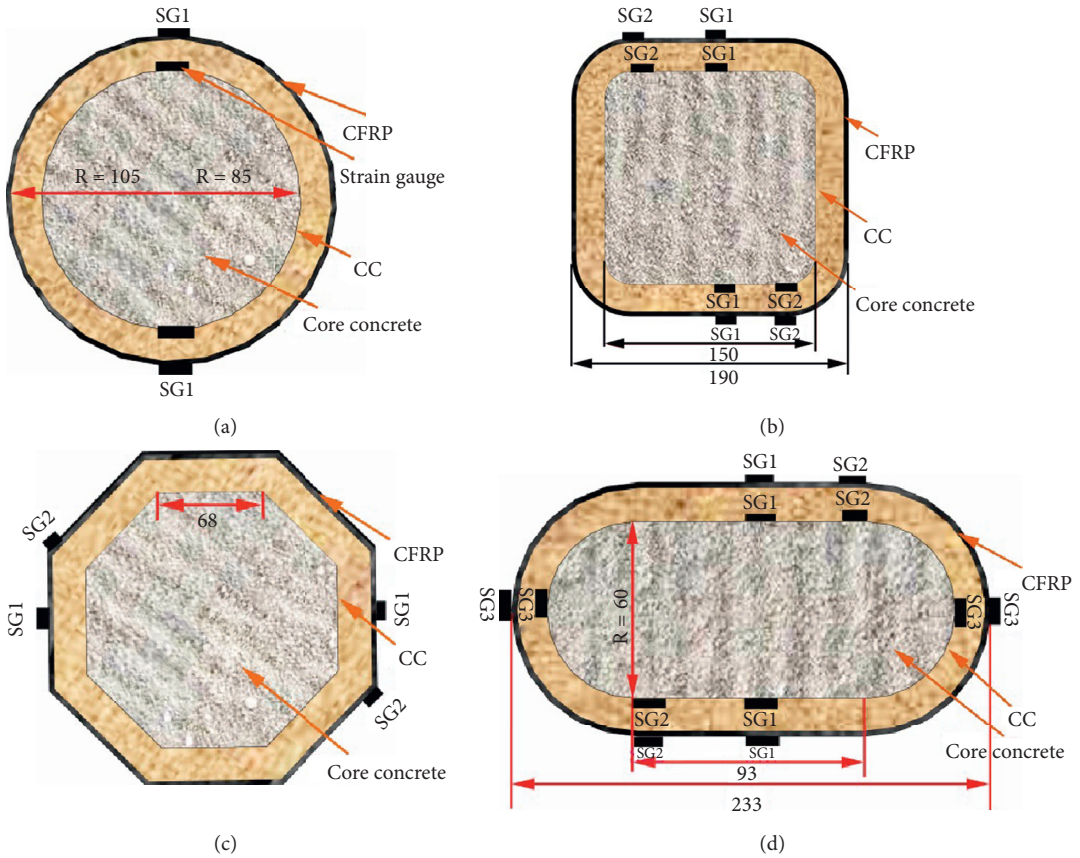

Figure 1: Schematic diagram of the reinforced column dimensions and strain gauge arrangement. (a) Circle. (b) Square. (c) Octagon. (d) Ellipse.

Figure 2: Molded test piece.

Table 2: Proportions of ingredients used for concrete mix.

Ingredients	w/c	Free water (kg/m^3)	Aggregate (kg/m^3)	River sand (kg/m^3)	Cement (kg/m^3)
Quantity	0.45	162	1 134	854	360

Table 3: Mechanical properties of CFRP.

Tensile strength, (MPa)	Modulus of elasticity (MPa)	Breaking elongation	Thickness per layer (mm)	Fiber weight (g·m^{-2})	Bending strength (MPa)
3547	2.33×10^5	1.61	0.167	294	734

Table 4: Mechanical Properties of epoxy resin.

Compressive strength (MPa)	Tensile strength (MPa)	Shear strength (MPa)	Elastic modulus (MPa)	Elongation (%)
82.7	57.8	22.39	2584.8	3

Table 5: Mechanical properties of concrete canvas.

Compressive strength (MPa)	Flexural strength (MPa)	Volumetric weight ($N \cdot m^{-3}$)
30.01	2.71	1249

schematic diagram of the concrete canvas is shown in Figure 3.

2.4. Instrumentation and Test Setup. By a testing machine with a maximal load capacity of 2500 kN, we experimented the samples overall in the case of concentric compression. Using an automatic data acquisition system, the strains of core concrete and CFRP, axial load, and vertical displacement were recorded for monitoring the samples' characteristics. For measuring the vertical displacement of the column in the mid-height region, as is shown in Figure 4, four linear variable displacement transducers (LVDTs) installed with a gauge length of 200 mm in each of the columns were employed. The full-height axial shortening was measured using two LVDT mounted at two opposite locations in the testing machine.

All of the samples underwent instrumenting process with strain gauges, glued either onto the concrete surface or onto the CFRP outer layer. The strain gauges were symmetrically mounted at multiple points at the mid-height of the specimens for measuring the strain in a range of locations. The gauge length of these strain gauges reached 5 mm. Figure 1 presents the transverse and axial strain gauges' locations, where SG 1 and SG 2 refer to middle positions on the side face and corner center, respectively. Before the formal loading of the specimen, the loading device is geometrically aligned with the specimen. The test procedure followed what is specified by the GB 50152–2012 standard [37]. The specimen is preloaded according to 15% of the estimated bearing capacity. At the initial stage, the load control mode is adopted. Before reaching the axial compressive strength of concrete, the load increment is 30 kN/min, and then, the displacement control mode is adopted. The speed is about 0.4 mm/min.

3. Results and Discussion

3.1. Failure Modes. The failure modes of overall enhanced concrete columns are presented in Figure 5. Noticeably, Figure 5 merely presents failure modes of taken samples as examples as the failing models have similarities to those in the respective group. Under expectation, only CFRP-wrapped columns failed by rupture of CFRP jacket as is shown in Figures 5(a)–5(d). For these column specimens, first, hear the click of epoxy cracking and then the sudden explosion of FRP cracking. The rupture of CFRP occurred at or near the middle height of the concrete, occurred outside the overlap zone, and occurred simultaneously with the crushing of the concrete and the sudden loss of load capacity. This is consistent with the experimental observations of some other researchers 23, 27, 28, 31, 32, 38]. Meanwhile, CFRP rupture of square and octagonal columns occurs at the corner first, which is in accordance with the experimental observations from some other researchers [27, 28, 32, 39]. CFRP rupture of the elliptic-like column occurs at the arc position. This phenomenon was also found in Teng 's research on fiber-reinforced concrete [38].

For columns wrapped with one-layer CC and CFRP, as is shown in Figures 5(e)–5(h), the failure position is similar to that only wrapped with CFRP, while it was worth finding that the fracture of CFRP is less serious than that of the former. The CFRP of the square column and octagonal column is broken in a thin strip-shaped failure mode. The CFRP of the elliptic column is broken in a villous failure mode. This was because the failure of CFRP was delayed after CC was adopted, which led to a substantial increase in the ductility of columns. In addition, the failure cross section of the column is close to the circular column after the application of CC, especially the octagon. This is probably because the cushion layer of CC makes the side closer to the circle, which makes the confinement more uniform. The CC can reduce the stress concentration of square and octagonal columns. The specimens confined with two layers CC and CFRP generally failed by CFRP failure, the failure mode of which is similar to that of specimens confined with one-layer CC as is shown in Figures 5(i)–5(l). However, the deformation of the specimen is larger before the failure of the specimen.

3.2. Load-Deformation Curve. The load-axial deformation curve can reflect the yield, strengthening, and deformation capacity of specimens under load. The load-axial deformation curve of the column only wrapped with CFRP for different cross-sectional shapes is plotted in Figure 6(a). From this figure, it is evident that the slope of the rising section of the curve increases in the order of square section, octagonal section, elliptical section, and circular section, indicating that the constraint stiffness is also increasing from square section to circular section. In addition, it can also be seen from the figure that the constraint strengthened phase of the elliptical column is the longest. The results are basically consistent with the literature [25, 27].

Comparing Figures 6(a) and 6(b), for the same cross-sectional shape, the stiffness of the specimen after adopted CC is significantly increased, and the bearing capacity and axial deformation are improved to a certain extent, especially for the circular and octagon shapes. After adding CC, CC can be regarded as an elastic-plastic cushion block, which improves the stress concentration at the corner of the specimen and makes the constraint of CFRP on the core concrete more uniform. The section shape of the octagonal column with CC is more close to the circle, and the improvement range is the largest. The above results show that CC can improve the stiffness and deformation ability of the specimen, especially for the specimen close to the circle, and improve the performance of the structure.

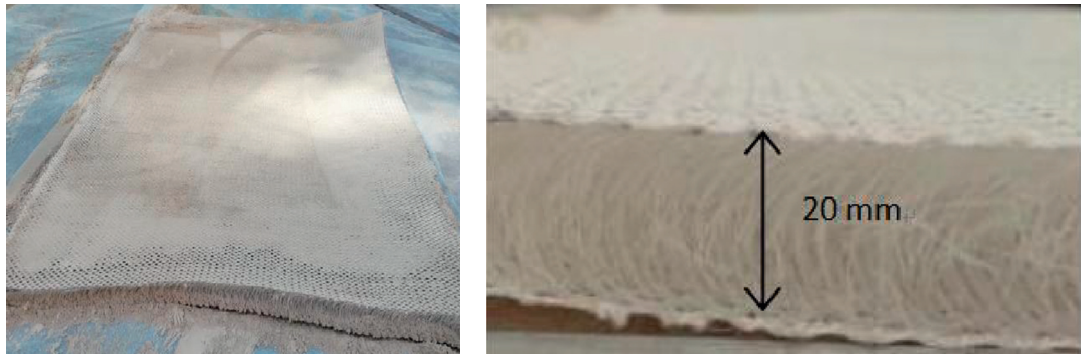

(a) (b)

Figure 3: Schematic diagram of the concrete canvas. (a) Concrete canvas filled with cement powder. (b) The size of 3D cc.

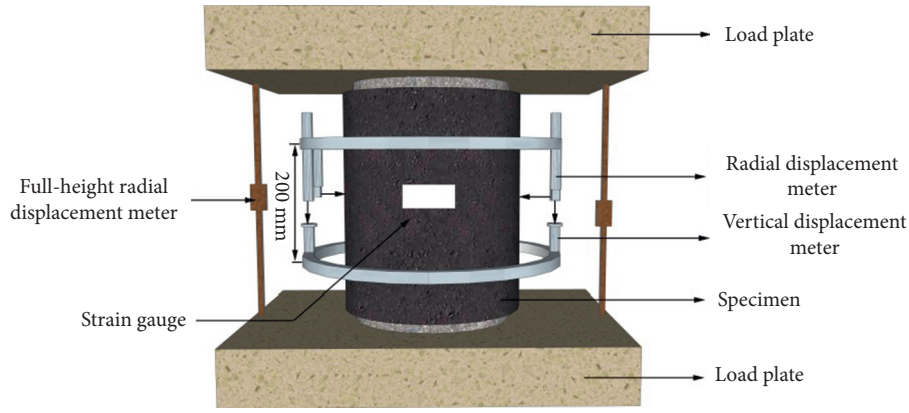

Figure 4: Test setup.

In addition, for specimens with different cross-sectional shapes, the bearing capacity and axial deformation change law of the specimens are similar to those in Figure 6(a). However, the change of the section shape from square column to circular column increases the stiffness and deformation ability of the specimen relative to the square column after CC is adopted. Among them, the octagonal column has the largest increase in the relative square column. The result indicates that CC can improve the increased amplitude of stiffness and deformation capacity of other cross-sectional shapes compared with the square column, and the increased amplitude of the specimen close to the circle is the largest.

Figure 6(c) shows the load-axial deformation curve of the reinforcement column wrapped with 2-layer CC. Compared with 1-layer CC, the increase of the slope of the curve is small, but the length of the strengthening stage is significantly increased. At the beginning of the test, the effect of external restraint on the core concrete is not obvious, and the slope of the curve does not change much. However, after entering the strengthening section, the elastic-plastic cushion block effect of the middle CC layer further increases due to the increase of the number of CC layers, the stress concentration of the specimen is further improved, and the load holding platform of the test piece increases. The above results show that increasing the number of CC layers can significantly improve the strengthening section of the specimen, can increase the load holding capacity and ultimate axial deformation of the specimen, but has little effect on the stiffness of the specimen.

3.3. Bearing Capacity Analysis. Table 6 gives the peak load of each group of specimens. N_u is the peak load of each group of specimens; ρrepresents the bearing capacity ratio of other section-shaped columns to square columns in the same CC layers. The peak load rises in the order of square, ellipse, octagon, and circle for the same CC layers (see Figure 7(a)). The peak load of the octagonal column, circular column, and elliptical column is 6%, 19%, and 5% higher than that of the square column for specimens only wrapped with CFRP. This order is due to the different constraint effects of CFRP on columns with different cross sections, among which the circular column has the best constraint effect, and the square column has the worst constraint effect. It is worth noting that as the number of CC layers increases, the ratio of the bearing capacity to the square column for the same cross section increases, indicating that after the use of CC, the side surface is closer to the arc shape so that the stress is more uniform when CFRP restrains it. Meanwhile, the bearing capacity of columns with the same cross-sectional shape shows an increasing trend as CC layers increase (see Figure 7(a)). The increase of peak load is 10.25%, 15.47%,

Figure 5: Failure mode of column. (a) S-0-1. (b) O-0-1. (c) C-0-1. (d) E-0-1. (e) S-1-1. (f) O-1-1. (g) C-1-1. (h) E-1-1. (i) S-2-1. (j) O-2-1. (k) C-2-1. (l) E-2-1.

10.37%, and 6.88% for square, octagon, circle, and ellipse, respectively, as CC layers increase from zero to two layers. This is mainly because CC can absorb energy as an elastic cushion through its distortion to improve the peak load of columns when they are damaged. In addition, note that the octagon has the biggest increasing amplitude, reaching 15.47%. This is mainly because the use of CC makes the octagonal cross-sectional column closer to the circular cross-sectional column, and the constraint effect is significantly improved. Compared with the specimens strengthened with one-layer CC, the bearing capacity of the specimens strengthened with two layers of CC increased to a certain extent, but the increased amplitude was not significant.

3.4. Ductility of the Test Piece. Ductility refers to a critical variable in terms of structural members because it elucidates the energy absorption and deformability of structural members in the course of failure. Ductility can be assessed by the ductility ratio μ, which is defined as the ultimate displacement Δu divided by the yield displacement Δy, that is, $\mu = \Delta u/\Delta y$ [34]. For the ductility in the present paper, μrepresents the ductility coefficient of the columns for different cross-sectional shapes. ξ represents the ductility coefficient ratio of the combined reinforced columns with different CC layers to the unconstrained columns. ξ° represents the ductility coefficient ratio of other section-shaped columns to square columns under the same CC layers. It can

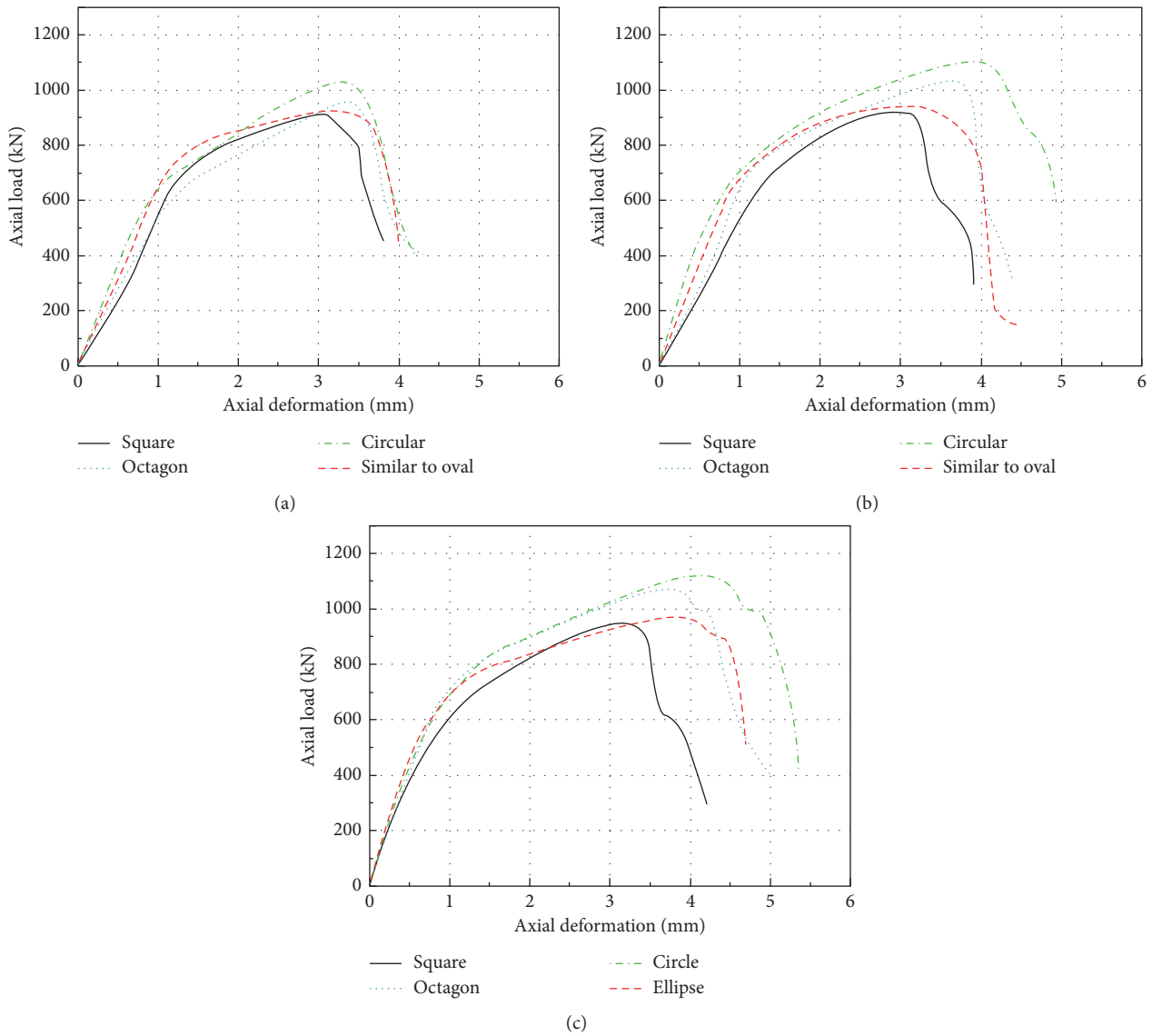

Figure 6: Load versus deformation relationship of specimens. (a) CFRP reinforcement. (b) One-layer CC and CFRP reinforcement. (c) Two-layer CC and CFRP reinforcement.

be seen from Table 6 that the ductility coefficient of specimens for the same CC layers changes with the change of the cross section. Among them, the ductility coefficient of the square column is the smallest, and that of the circular column is the largest, followed by the octagon column and ellipse column (see Figure 8(a)). As the number of CC layers increases, the ductility coefficient ratio of other section-shaped columns to square columns shows a decreasing trend. Among them, the circular shape decreases the most, and the octagonal shape decreases the least, indicating that changing the cross-sectional shape can improve the ductility, and adopting CC can improve the ductility of the octagon best. Meanwhile, it can be observed that the displacement ductility coefficient for the same section shows an increasing trend as CC layers increase. The increase of ductility is 56%, 40.0%, 22.5%, and 33.3% for square, octagon, circle, and ellipse, respectively, as CC layers increase from zero to two layers. It is worth noting that the ductility of the square column increased the most, but the ductility of the circular column increased very little. This is mainly because CC can absorb energy as an elastic cushion through its distortion to improve the ductility of columns when they are damaged. The above result further indicated that CC can obviously improve the defect of stress concentration at the corner of the column especially the square.

3.5. Stress versus Strain Relationship. Table 6 gives the stress and strain value of each group of specimens. f_{cc}' is the peak stress corresponding to the peak load of constraining concrete column; f_{co}' is the peak stress corresponding to the peak load of the unconstraining concrete column; ε_{cc} is the longitudinal strain of the concrete surface corresponding to the peak load of constraining concrete column; ε_{co} is the

Table 6: Peak load and stress of each group of specimens.

Specimen	CC layer	N_u (kN)	ρ	f_{cc}' (MPa)	$\frac{f_{cc}'}{f_{co}'}$	ε_{cc}	$\frac{\varepsilon_{cc}}{\varepsilon_{co}}$	μ	ξ	ξ°
S-0-0	0	800.36	1.00	34.69	1.00	2 130	1.00	1.12	1.00	1.00
O-0-0		728.57	0.93	32.38	1.00	2 200	1.00	1.41	1.00	1.17
C-0-0		802.32	1.03	35.66	1.00	2 280	1.00	1.65	1.00	1.31
E-0-0		740.36	0.95	32.90	1.00	2 170	1.00	1.30	1.00	1.13
S-0-1	0	920.00	1.00	40.89	1.18	4 250	2.00	2.5	2.23	1.00
O-0-1		976.86	1.06	43.42	1.34	5 325	2.42	3.2	2.26	1.28
C-0-1		1 091.16	1.19	48.50	1.36	5 945	2.61	4.0	2.42	1.60
E-0-1		962.00	1.05	42.76	1.30	4 638	2.14	3.0	2.30	1.20
S-1-1	1	984.40	1.00	43.75	1.26	5 830	2.74	3.7	3.30	1.00
O-1-1		1 094.08	1.11	48.63	1.50	7 055	3.21	4.3	3.04	1.16
C-1-1		1 178.45	1.20	52.38	1.47	7 745	3.40	4.7	2.85	1.27
E-1-1		1 010.00	1.03	44.89	1.36	6 258	2.88	3.8	2.92	1.03
S-2-1	2	1 004.09	1.00	44.62	1.29	6 436	3.02	3.9	3.48	1.00
O-2-1		1 128.00	1.12	50.13	1.55	7 481	3.40	4.5	3.18	1.15
C-2-1		1 204.38	1.20	53.53	1.50	7 961	3.50	4.9	2.96	1.26
E-2-1		1 028.18	1.02	45.70	1.39	6 782	3.13	4.0	3.08	1.05

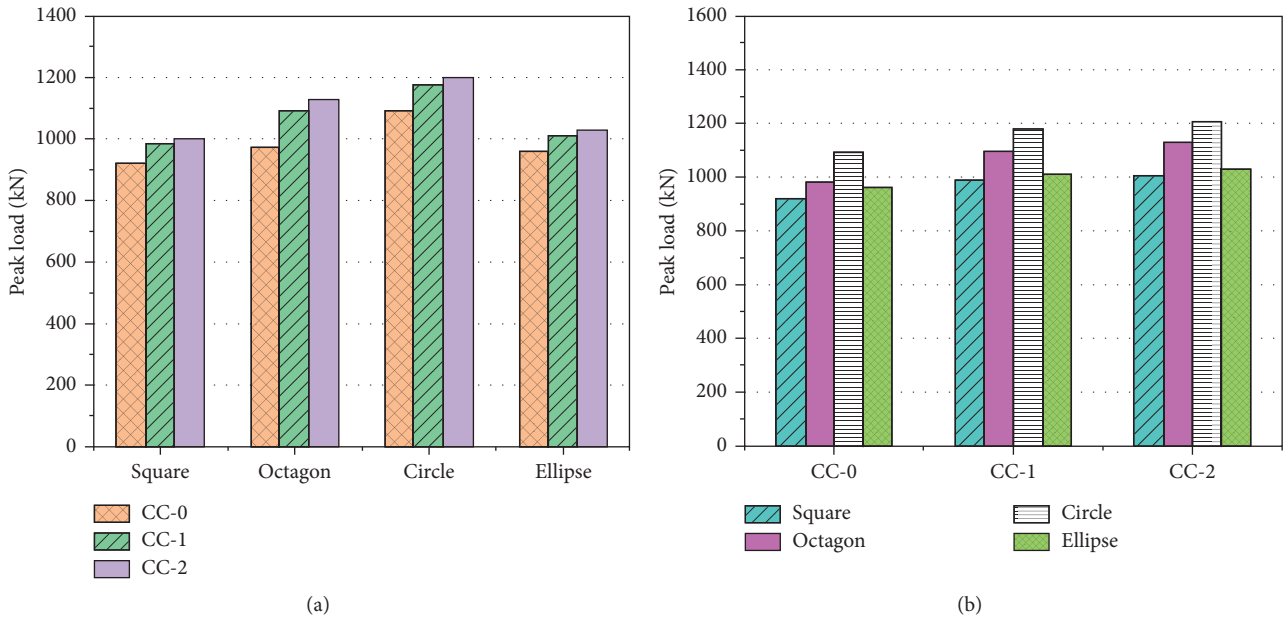

Figure 7: The peak load of the columns with different cc layers and cross-sectional shape. (a) CC layers. (b) Cross-sectional shape.

longitudinal strain corresponding to the peak load of the unconstraining concrete column; f_{cc}'/f_{co}' is the constraint strength ratio. The constraint strength and peak strain of circular section specimens are the largest for the same number of CC layers. The peak strain increases with the increase of the number of CC layers for the columns with the same section shape, which indicates that the constraint strength of CFRP to the core concrete becomes stronger after the addition of CC. With the increase of the number of CC layers, the constraint strength of octagonal columns increases the most. The reason may be that with the increase of the number of CC layers, the improvement effect of stress concentration of octagonal columns is better than that of other sections.

Figure 9 plots the strains for a range of cross-sectional shapes reinforced by CFRP and CC on a range of measuring point surfaces. In the present article, noticeably, the stress-strain curves are axial stress-hoops strain and axial stress-axial strain curves unless otherwise specified. In general, the stress-strain curve of each measuring point is identical to that of the rising section of the load-deformation curve, showing an approximately bilinear trend. The transverse strains for the intermediate position of the concrete surface strengthened by CFRP and by one-layer CC and CFRP are plotted in Figures 9(a) and 9(b), separately. From these figures, the transverse strain at the peak load of concrete surface increases in the order of circle, octagon, ellipse, and square, which indicates that the reinforcement effect will be significantly improved by changing the section shape. The sides of circular cross-sectional columns are relatively uniform, and CC and CFRP can exert their restraining ability to a greater extent. Noticeably, the concrete surface

transverse strains at peak load for the same cross-sectional shape increased remarkably from CC wrap to CC and CFRP wrap as is shown in Figures 9(a) and 9(b) which show that CC can improve the CFRP constraint effect and reduce the transverse strain of concrete. Therefore, the reason for the bearing capacity of the CC and CFRP confined members tested under axial compressive loading tests being noticeably enhanced is interpreted (Figure 7 and Table 6).

In order to study the influence of different section shapes and CC layer numbers on the strain of CFRP, the strains for the intermediate position of CFRP surface strengthened by CFRP and by one-layer CC and CFRP are plotted in Figures 9(c) and 9(d), respectively. In terms of stress-strain curves in the present article, the following sign convention is adopted: transverse strains are positive, and longitudinal strains are negative. The stress-strain curves in Figures 9(c) and 9(d) are overall shown in line with the axial stress-axial strain curve presented on the right while the axial stress-hoop strain curve presented on the left. Notably, strains at peak load of elliptical, square, and octagonal shapes are similar after adopting CC, except for the maximum strain of circular section. This follows the data presented in Figure 8, where higher ductility gain was also recorded after adopting CC. For the specimens only wrapped with CFRP and one-layer CC and CFRP, the stress and strain of circular column are maximum value compared with the square column, followed by octagonal column and elliptical column, mainly because the constraint of external reinforcement on the circular column is more uniform than that of the square column, octagonal column, and elliptical column. Nevertheless, with the increase of the number of CC layers, the stress increased degree of circular columns decreases compared with that of square columns, while the increased degree of octagonal columns increases. This phenomenon is consistent with the data in Figure 7 and Table 6. The main reason is that when two layers of CC are strengthened, the side of octagonal columns is closer to that of circular columns, so that the external reinforcement can restrain them more evenly. Furthermore, the CFRP strains at peak load for the same cross-sectional shape increased by comparison remarkably as is also shown in Figures 9(c) and 9(d).

In order to study the role of CC in strengthening specimens, the strain on the CFRP surface was compared with that on the concrete surface corresponding to the same position. The transverse strain difference between the fiber surface and the concrete surface at the middle of the CC and CFRP column (when the fiber strain is greater than the concrete strain) was plotted in Figure 9(e). For stress-strain curves in the present paper, the abscissa is the transverse strain difference between fiber and concrete. From this figure, it can be seen that the strain difference between the fiber and the concrete for all cross-sectional shape columns is very close When the stress is in the range of 20–38 MPa, this indicates that the influence of CC on columns with different cross sections is not different. However, it is worth noting that the strain difference between the fiber and the concrete increases in the order of square, ellipse, octagon, and circle when the stress increases.

In order to study the improvement of CC on corner restraint of specimens, the transverse strains of the square and octagonal columns for different positions of CFRP surface strengthened by CFRP and by CC and CFRP are plotted in Figures 9(f) and 9(g), respectively. For stress-strain curves in the present article, No.1 (CFRP) represents the strain at the CFRP surface in the middle of the CFRP-wrapped column; No.2 (CFRP) represents the strain at the CFRP surface at the corner of the CFRP-wrapped column; No.1 (CC and CFRP) represents the strain at the CFRP surface in the middle of the CC and CFRP-wrapped column; No.2 (CC and CFRP) represents the strain at the CFRP surface at the corner of the CC and CFRP-wrapped column as is shown in Figure 2. From these figures, the strain at the corner is significantly higher than the strain at the middle position. Noticeably, the difference between the strain at the corner and the intermediate position for the same cross-sectional shape is significantly reduced after the CC is adopted, which indicates that CC can reduce the stress concentration at the corners. This also follows the data presented in Figure 6 where, under the same cross-sectional shape, the members wrapped with CC and CFRP exhibited better ductility gain than those only wrapped with CFRP. Besides, Whether CFRP reinforcement or CC and CFRP reinforcement, the strain difference at the two positions of the octagonal column is smaller than that of the square column, which can improve the corner stress concentration better than other cross-sectional columns.

The transverse strains of the elliptical and circular columns for different positions of CFRP surface strengthened by CC and CFRP are plotted in Figure 9(h), respectively. For stress-strain curves in the present paper, No.1 (sto) represents the strain at the CFRP surface in the middle of the CFRP and CC wrapped elliptical column; No.2 (sto) represents the strain at the CFRP surface at the corner of the CC and CFRP-wrapped elliptical column; No.3 (sto) represents the strain at the CFRP surface at the arc of the CC and CFRP-wrapped elliptical column (Figure 2). From this figure, the strain of the elliptical column increases in order according to the intermediate, the corner, and the arc of the column. This can be explained by the fact that the arc of the column subjected better restraining effects than other positions. Notably, the strain of the CFRP surface at the arc of the elliptical column is higher than that of the circular column. This is due to the nonuniform constraint of the elliptical section column, and the constraint effect is better in the arc position.

Generally speaking, the stress concentration of columns with different cross-sectional shapes is greatly improved by using CC compared with only wrapped CFRP columns. In particular, for the square column, because of its irregularity, the corner restraint is stronger than the middle part, and there are strong and weak restraint areas, as shown in Figure 10(a). After using CC, due to the cushion effect of CC, the constraint is more uniform, as shown in Figure 10(b). Through comparing constraint effect drawings of two different constraint forms, the effective confinement zone increases and the invalid restraint zone decreases after CC is used, such as 10(c).

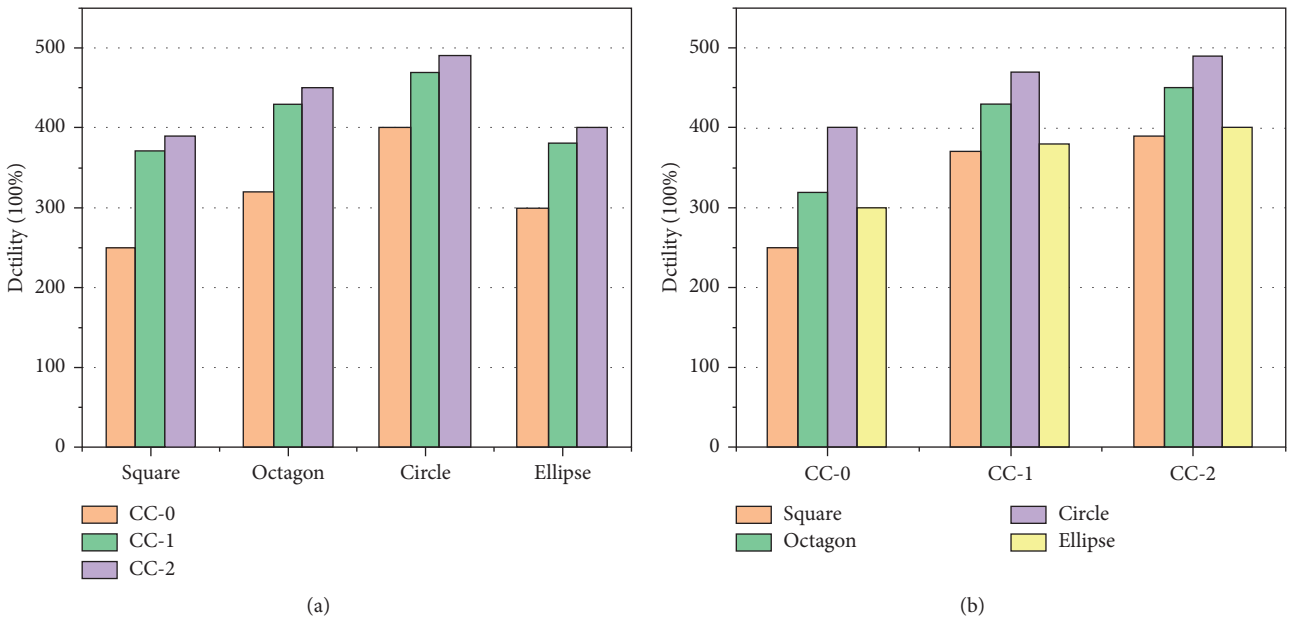

Figure 8: The ductility of the columns with different cross-sectional shapes and CC layers. (a) Cross-sectional shape. (b) CC layers.

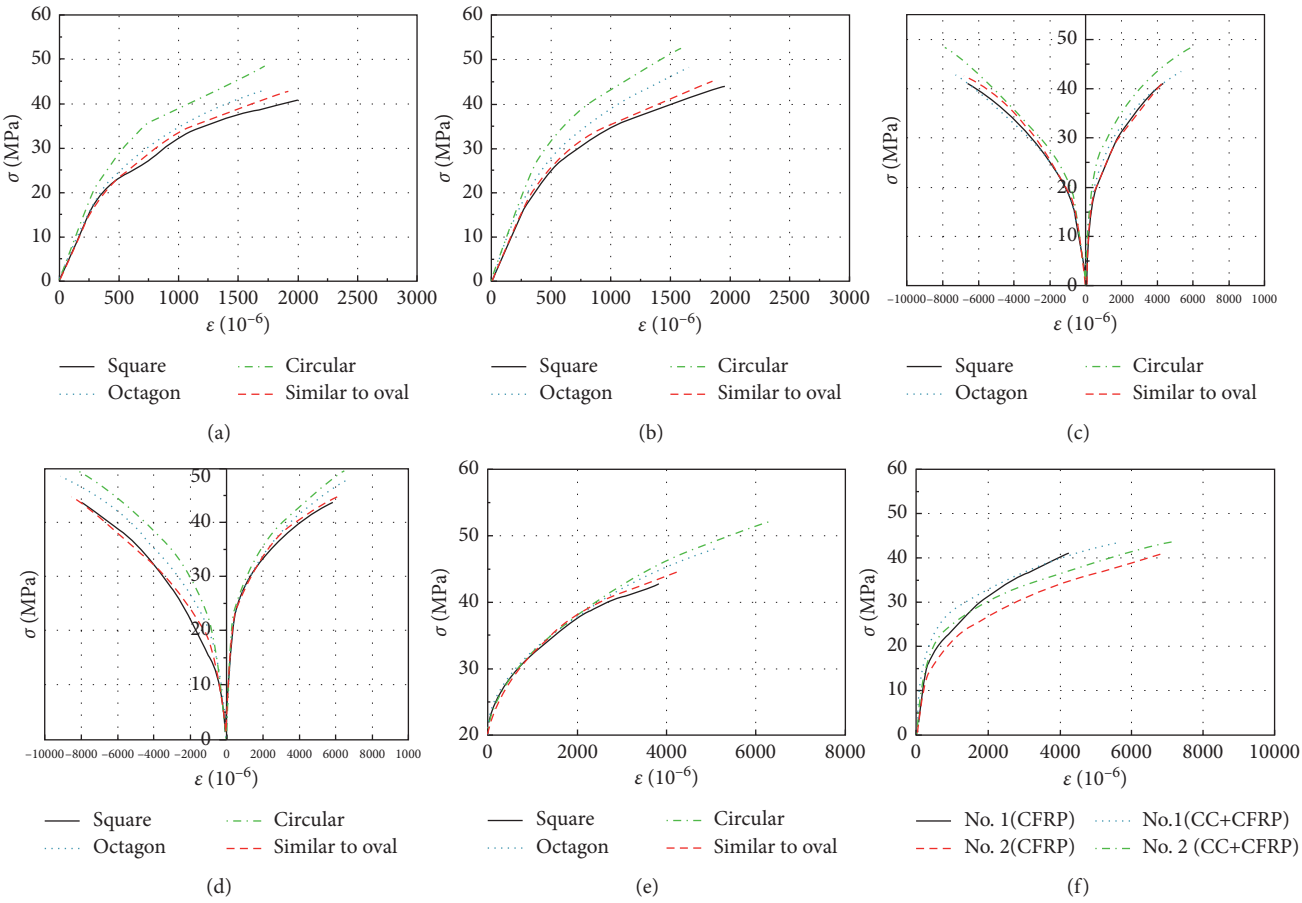

Figure 9: Continued.

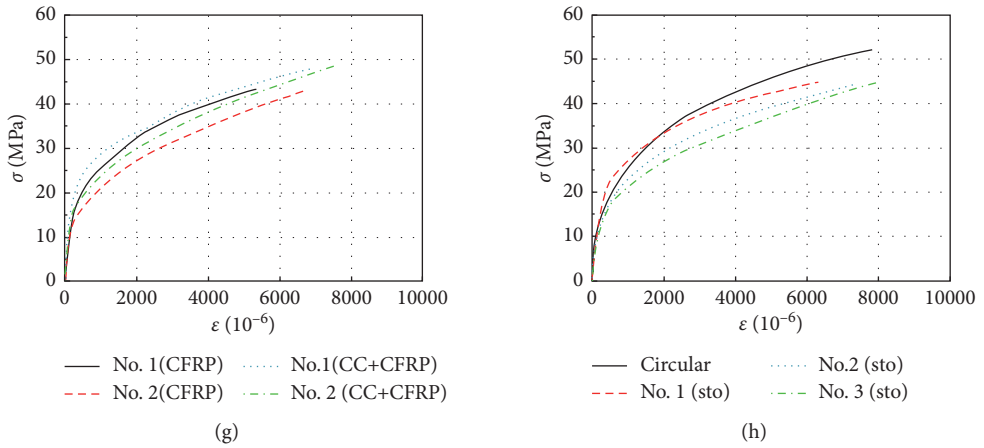

Figure 9: The stress-strain curves. (a) CFRP-reinforced column concrete surface. (b) CC and CFRP-reinforced column concrete surface. (c) CFRP-reinforced column fiber surface. (d) CC and CFRP-reinforced column fiber surface. (e) Strain difference between fiber and the concrete surface. (f) Strain at different positions on a square column. (g) Strain at different positions of the octagonal column. (h) Strain at different positions of the circular and the elliptical columns.

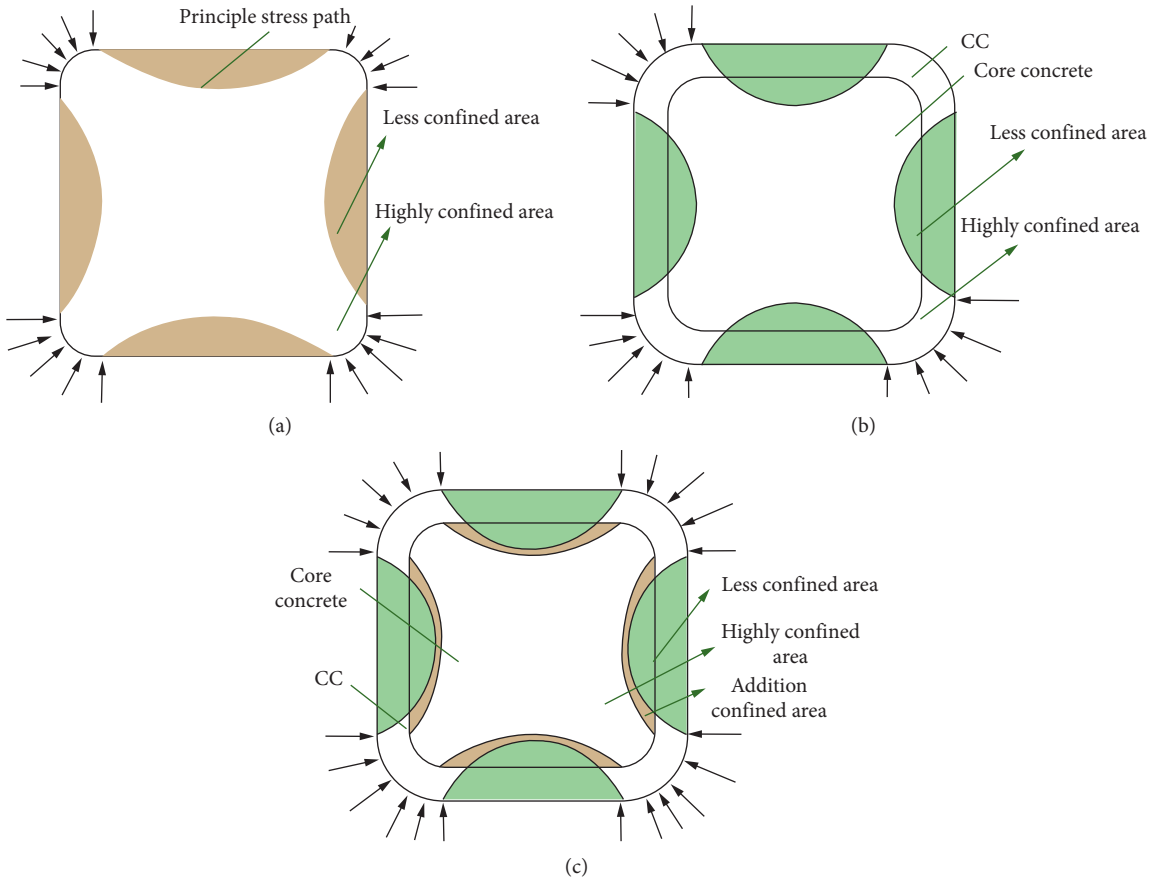

Figure 10: Schematic diagram of the confined area with different methods. (a) CFRP-reinforced column. (b) CFRP and concrete canvas-reinforced column. (c) The different confined areas with the two reinforced methods.

4. Conclusion

This study presents an experimental investigation of the behavior of axially loaded short columns with different cross-sectional shape strengthened with CC and CFRP wrap. The main purpose was to investigate the effect of the cross-sectional shapes and CC layers on the columns reinforced by CC and CFRP jackets. Two parameters were considered:

cross-sectional shapes (circle, octagon, ellipse, and square) and the number of CC layers (zero, one, and two). Comparing and discussing processes in the present article lead to the following conclusions:

(1) For columns wrapped with one-layer CC and CFRP, the failure position is similar to that only wrapped with CFRP. However, the fracture of CFRP is less serious than that of the former. Moreover, the deformation of the specimen increases obviously, and the brittleness of the specimen is improved obviously. In addition, the column's failure cross section is close to the circular one after the application of CC, especially the octagon. Using CC can obviously reduce the brittle failure of the specimens.

(2) The bearing capacity of specimens wrapped with CC and CFRP is greater than that of specimens only wrapped with CFRP. However, the bearing capacity of the octagonal section column wrapped with CC and CFRP is increased by 15.47%, which is the maximum of four cross-sectional shapes. Adopting CC can improve the bearing capacity of the column only strengthened by CFRP, and the bearing capacity of the specimen whose cross-sectional shape is close to the circular one is the largest.

(3) Compared with the only CFRP-wrapped columns, the ductility coefficients of adopting two-layer CC columns increased by 56%, 40%, 22.5%, and 32.6% for the square, octagonal, elliptical, and circular columns, respectively. The square column has the largest increase range, while the circular column has the smallest increase range. CC can effectively improve the ductility of irregular sections, but it has little effect on the round specimen.

(4) With the increase of the CC layer, the constraint strength ($f_{cc}^{'}/f_{co}^{'}$) of the octagonal column increases by 155% at most. With the increase of the number of CC layers, the stress increased degree of circular columns decreases compared with that of square columns, while the increased degree of octagonal columns increases. The stress concentration of columns with different cross-sectional shapes is greatly improved by using CC compared with only wrapped CFRP columns, especially for the square column. At the same time, due to the existence of CC, the stress concentration phenomenon of CFRP is greatly improved, and the utilization rate of the ultimate strain of CFRP is increased.

Future work is required to develop a more sophisticated stress-strain model for CC and CFRP-confined columns with different cross-sectional shapes. Meanwhile, further experimental investigations could use intermittent hoop wraps instead of full wrapping of specimens.

Data Availability

The data used to support the findings of this study are available from the corresponding author upon request.

Conflicts of Interest

The author claims that there are no conflicts of interest.

Authors' Contributions

Jiangang Niu contributed to the investigation, funding acquisition, and project administration; Wenming Xu, data curation, methodology, validation, formal analysis, and writing the original draft; Jingjun Li, writing the original draft, reviewing, editing, and supervision; Jian Liang, reviewing, editing, and visualization. All authors have read and agreed to the published version of the manuscript.

Acknowledgments

This study was financed by the National Natural Science Foundation of China (grant no. 51968058), Natural Science Foundation granted by the Department of Education and supported by the Program for Young Talents of Science Technology in University of Inner Mongolia Autonomous Region (grant no. NJYT-18-A06). This work was also supported by the Inner Mongolia Autonomous Region Talent Development Foundation.

References

[1] Q. Cao, J. Zhou, R. Gao, and Z. J. Ma, "Flexural behavior of expansive concrete beams reinforced with hybrid CFRP enclosure and steel rebars," *Construction and Building Materials*, vol. 150, pp. 501–510, 2017.

[2] P. Sadeghian, A. R. Rahai, and M. R. Ehsani, "Experimental study of rectangular RC columns strengthened with CFRP composites under eccentric loading," *Journal of Composites for Construction*, vol. 14, no. 4, pp. 443–450, 2010.

[3] A. B. B. Abu-Sena, M. Said, M. A. Zaki, and M. Dokmak, "Behavior of hollow steel sections strengthened with CFRP," *Construction and Building Materials*, vol. 205, pp. 306–320, 2019.

[4] E. Hamed and O. Rabinovitch, "Lateral out-of-plane strengthening of masonry walls with composite materials," *Journal of Composites for Construction*, vol. 14, no. 4, pp. 376–387, 2010.

[5] A. Saljoughian, D. Mostofinejad, and S. M. Hosseini, "CFRP confinement in retrofitted RC columns via CSB technique under reversed lateral cyclic loading," *Materials and Structures*, vol. 52, no. 4, 67 pages, 2019.

[6] Q. Xie, H. Sinaei, M. Shariati, M. Khorami, and D. T. Bui, "An experimental study on the effect of CFRP on behavior of reinforce concrete beam column connections," *Steel and Composite Structures*, vol. 5, no. 30, pp. 433–441, 2019.

[7] H. Sinaei, M. Z. Jumaat, and M. Shariati, "Numerical investigation on exterior reinforced concrete Beam-Column joint strengthened by composite fiber reinforced polymer (CFRP)," *Steel and Composite Structures*, vol. 28, no. 6, pp. 433–441, 2011.

[8] A. Saljoughian and D. Mostofinejad, "Grooving methods in square RC columns strengthened with longitudinal CFRP under cyclic axial compression," *Engineering Structures*, vol. 52, pp. 724–735, 2019.

[9] S. A. Hadigheh, R. J. Gravina, and S. T. Smith, "Effect of acid attack on FRP-to-concrete bonded interfaces," *Construction and Building Materials*, vol. 152, pp. 285–303, 2017.

[10] A. Abaniliam, Y. Li, and V. M. Karbhari, "Durability characterization of wet layup graphite/epoxy composites used in external strengthening," *Composites Part B: Engineering*, vol. 37, pp. 200–212, 2006.

[11] K. Soudki, E. El-Salakawy, and B. Craig, "Behavior of CFRP strengthened reinforced concrete beams in corrosive environment," *Journal of Composites for Construction*, vol. 11, no. 3, pp. 291–298, 2007.

[12] Y. J. Kim and Y. Ji, "Axial load-bearing concrete confined with carbon fiber-reinforced polymer sheets in acidic environment," *ACI Structural Journal*, vol. 114, no. 3, pp. 775–786, 2017.

[13] O. Ali, D. Bigaud, and E. Ferrier, "Comparative durability analysis of CFRP-strengthened RC highway bridges," *Construction and Building Materials*, vol. 228, Article ID 116756, 2019.

[14] Y. Yongming, G. A. Manuel, H. Silva, and C. Biscaia, "Bond durability of CFRP laminates-to-steel joints subjected to freeze-thaw," *Composite Structures*, vol. 212, pp. 243–258, 2019.

[15] O. Khalafalla, M. Pour-Ghaz, A. Elsafty, and S. Rizkalla, "Durability of CFRP strands used for prestressing of concrete structural members," *Construction and Building Materials*, vol. 228, Article ID 116756, 2019.

[16] F. Han, H. Chen, X. Li et al., "Improvement of mechanical properties of concrete canvas by anhydrite-modified calcium sulfoaluminate cement," *Journal of Composite Materials*, vol. 50, no. 14, pp. 1937–1950, 2016.

[17] F. Han, H. Chen, K. Jiang, W. Zhang, T. Lv, and Y. Yang, "Influences of geometric patterns of 3D spacer fabric on tensile behavior of concrete canvas," *Construction and Building Materials*, vol. 65, pp. 620–629, 2014.

[18] G. Pamuk, F. Ceken, B. M. Bulent Murat Icten, and R. Karakuzu, "Mechanical properties of spacer fabric-reinforced composites knitted from glass yarn," *Journal of Composite Materials*, vol. 45, no. 17, pp. 1741–1748, 2011.

[19] L. Zhou, G. Ding, J. Tan, X. Zhao, and J. Wang, "Seismic response of concrete-canvas reinforced slopes: influence of tilt degrees for reinforcement," *Journal of Earthquake and Tsunami*, vol. 1, no. 14, p. 26, 2019.

[20] H. Li, H. Chen, X. Li, and F. Zhang, "Design and construction application of concrete canvas for slope protection," *Powder Technology*, vol. 344, pp. 937–946, 2019.

[21] F. Zhang, H. Chen, X. Li et al., "Experimental study of the mechanical behavior of FRP-reinforced concrete canvas panels," *Composite Structures*, vol. 176, pp. 608–616, 2017.

[22] Z. Meng, Y. F. Hu, J. G. Zhang, W. Ye, and M. M. Zhao, "Crashworthiness of CFRP/aluminum alloy hybrid tubes under quasi-static axial crushing," *Journal of Materials Research and Technology*, vol. 9, no. 4, pp. 7740–7753, 2020.

[23] J.-J. Zeng, Y.-C. Guo, W.-Y. Gao, W.-P. Chen, and L.-J. Li, "Stress-strain behavior of concrete in circular concrete columns partially wrapped with FRP strips," *Composite Structures*, vol. 200, pp. 810–828, 2018.

[24] T. E. Maaddawy, M. E. Sayed, and B. Abdel-Magid, "The effects of cross-sectional shape and loading condition on performance of reinforced concrete members confined with Carbon Fiber-Reinforced Polymers," *Materials and Design (1980-2015)*, vol. 31, no. 5, pp. 2330–2341, 2010.

[25] W.-C. Hwang, Y.-J. Yang, C.-S. Cha et al., "Impact collapse behavior of CFRP structural members according to the variation of section shapes and stacking angles," *International Journal of Precision Engineering and Manufacturing*, vol. 16, no. 4, pp. 677–684, 2015.

[26] D. A. Moran and C. P. Pantelides, "Elliptical and circular FRP-confined concrete sections: a Mohr-Coulomb analytical model," *International Journal of Solids and Structures*, vol. 49, no. 6, pp. 881–898, 2012.

[27] I. P. Vipulkumar, U. K. A. P. Brian, and A. Farhad, "Confined concrete model of circular, elliptical and octagonal CFST short columns," *Steel and Composite Structures*, vol. 22, pp. 497–520, 2003.

[28] S. Saleem, Q. Hussain, and A. Pimanmas, "Compressive behavior of PET FRP–confined circular, square, and rectangular concrete columns," *Journal of Composites for Construction*, vol. 3, no. 21, pp. 1–18, 2016.

[29] D. Mostofinejad, N. Moshiri, and N. Mortazavi, "Effect of corner radius and aspect ratio on compressive behavior of rectangular concrete columns confined with CFRP," *Materials and Structures*, vol. 1-2, no. 48, pp. 107–122, 2015.

[30] Z. Yan and C. P. Pantelides, "Concrete column shape modification with FRP shells and expansive cement concrete," *Construction and Building Materials*, vol. 25, no. 1, pp. 396–405, 2011.

[31] L.-M. Wang and Y.-F. Wu, "Effect of corner radius on the performance of CFRP-confined square concrete columns: Test," *Engineering Structures*, vol. 30, no. 2, pp. 493–505, 2008.

[32] Y. A. Al-Salloum, "Influence of edge sharpness on the strength of square concrete columns confined with FRP composite laminates," *Composites Part B: Engineering*, vol. 38, no. 5-6, pp. 640–650, 2007.

[33] O. A. Farghal, "Structural performance of axially loaded FRP-confined rectangular concrete columns as affected by cross-section aspect ratio," *HBRC Journal*, vol. 14, no. 3, pp. 264–271, 2019.

[34] M. T. Jameel, M. N. Sheikh, and M. N. S. Hadi, "Behaviour of circularized and FRP wrapped hollow concrete specimens under axial compressive load," *Composite Structures*, vol. 171, pp. 538–548, 2017.

[35] ASTM D3039/D3039M-17, *Standard Test Method for Tensile Properties of Polymer Matrix Composite Materials*, China Architecture and Building, Beijing, China, 2008.

[36] JGJ/T 70—2009, *Standard for Test Method of Performance on Building Mortar*, China Architecture and Building Press, Beijing, China, 2009.

[37] GB 50152—2012, *Standard for Test Method of Concrete Structures*, China Architecture and Building Press, Beijing, China, 2012.

[38] J. G. Teng and L. Lam, "Compressive behavior of carbon fiber reinforced polymer-confined concrete in elliptical columns," *Journal of Structural Engineering*, vol. 128, no. 12, pp. 1535–1543, 2002.

[39] J.-H. J. Kim, S.-T. Yi, S.-H. Lee, S.-K. Park, and J.-K. Kim, "Compressive behaviour of CFS strengthened concrete specimens with various cross-sectional shapes and laminations," *Magazine of Concrete Research*, vol. 55, no. 5, pp. 407–418, 2003.